EFFECTS OF CURRENT RIPPLE ON DEAD-TIME DISTORTION IN THREE-PHASE VOLTAGE SOURCE INVERTERS

Gabriele Grandi [1], *Jelena Loncarski* [1], *Roland Seebacher* [2]

[1] Department of Electrical Engineering, University of Bologna, Italy
[2] Technical University of Graz, Austria

ABSTRACT

Inverter dead-time distortion in output voltages have been widely investigated in the past for three-phase PWM voltage source inverters. Also, there have been some studies about multi-phase inverters with reference to multi-phase drives. Usually, almost sinusoidal output currents are considered, with a single zero crossing for every half fundamental period. High output current ripple introduces multiple zero crossing, leading to modified output voltage distortions. In this paper the effect of the output current ripple has been taken into account, in the case of carrier-based PWM techniques when no any dead-time compensation technique is applied. In particular, the harmonic spectrum of the output voltage distortion has been evaluated on the basis of the multiple zero crossing time interval of output currents. In case of relevant current ripple it is verified a relevant deviation of output voltage harmonics in comparison to the case of almost sinusoidal currents. Theoretical analysis has shown that particular low-order harmonics are affected by the current ripple amplitude, and simulation results confirm the developed analytical approach.

Index Terms**—** *Switch dead-time, zero crossing, current ripple, harmonic analysis, inverter nonlinearity.*

1. INTRODUCTION

Pulse-width modulation inverters have widely been used in motor drives. However, these inverters produce voltage distortion due to nonlinear characteristics of switching devices such as turn-on/turn-off times, voltage drops on switches and diodes. A further important nonlinearity is caused by necessary dead-time introduced to avoid the so-called shoot-through of the dc link. In fact, to guarantee that both switches never conduct simultaneously, a small time delay is applied to the gate signal of the turning on device. This small time interval, in order of μs, introduces magnitude and phase errors in the output voltage. The voltage distortion increases with switching frequency, introducing harmonic components that may cause instabilities and additional losses in the machine being driven. Relative voltage deviation effect is more significant for low modulation indexes [1]-[5].

The dead-time problem has already been investigated by the industry [2], [3] and various solutions have been proposed. In most cases the compensation techniques are based on an average value theory, the lost volt-seconds are averaged over an entire switching period and added to the commanded value. A pulse-based compensation method has been proposed in [2], where the compensation is realized for each pulse. The compensation voltages in [3] are calculated by using dead-time, switching period, current command and dc-link voltage. Regardless of the method used, all dead-time compensation techniques are based on polarity of the current in the switching leg. This is especially true around the zero crossing where an accurate measurement is needed to correctly compensate for the dead-time. In [4] an online dead-time compensation technique is presented, acquiring the additional computation burden to determine the phase angle of currents.

The area of multiphase variable-speed motor drives, in general, and multiphase induction motor drives, in particular, has experienced a substantial growth since the beginning of this century. Detailed overview of the current state-of-the-art in this area is given by [6]. The inverter dead-time effect on the steady-state and dynamic performances of a multi-phase induction machine with current control is analyzed in [7]. The paper suggests a modified current control scheme that is able to compensate inverter dead-time and provides sinusoidal currents. Although in this case it is possible to have perfect compensation of dead-times, the problem remains for the drives that are based on machine flux estimation, since dead-time introduces errors if input dc voltage and switch patterns are used for calculations instead of actual ac output voltages. Analysis and compensation method for a five-leg inverter driving two three-phase ac motors independently has been done in [8]. Practically, this analysis can be simplified as for three-phase inverters, since the motors are independent. An analysis of the effect of dead-time introduced for multi-phase inverters is given by [9], first for the case of three-phase, then with a general extension to n phases, with specific numerical verifications on five- and seven-phase inverters. An overview on dead-time analysis on multi-phase inverters is given as well in [10], where is the dead-time effect on load voltage also represented in terms of multiple space vectors, and analysis of harmonics content for each α-β plane is given.

978-1-4673-1454-1/12/$31.00

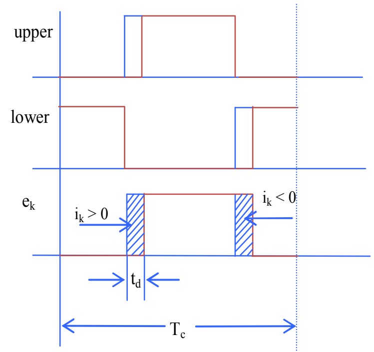

Fig. 1 Switching patterns and output pole voltage

Even though the compensation of dead-times can be done on the basis of current sign measurement, never it is perfect since the turn-on/turn-off times are not known exactly and are depending on many factors [11], leading to either an over-compensation or under-compensation.

Due to the multiple zero crossings, when the output current is with ripple, dead-time has different influence on output voltage, as well as on its harmonic spectrum. An analysis is given in [12], where is proposed a resonant controller to compensate for relevant harmonics introduced by dead-time.

In this paper a brief review of the dead-time effects in three-phase inverters is presented first, which is almost well known and investigated. Further on, the effect of multiple zero crossings of output current is introduced by analytical developments and verified with numerical simulations by a realistic circuit model.

2. REVIEW OF DEAD-TIME EFFECTS IN THREE-PHASE VSIs

Reference is made to a typical three-phase PWM voltage source inverter (VSI) with a passive RL balanced load. It is convenient to analyze the dead-time effects from one phase leg converter and then to extend the results to more legs (phases). During the dead-time t_d, both of the switching devices cease to conduct, and one of the two diodes conducts. If the current polarity is positive, the lower diode will conduct, otherwise the upper diode will conduct.

The corresponding switching patterns and output voltages are shown in Fig. 1. The ideal gating pattern is shown in blue color. However, in practical applications, the turn-on time of each switch is delayed by the dead-time t_d, leading to the real gating signals shown in red color.

The actual pole voltage of k-th leg (k = 1, 2, 3), e_k, can be evaluated on the basis of the reference pole voltage, e_k^*, according to the direction of the phase current i_k as:

$$e_k = e_k^* - sign(i_k)\Delta V_d \tag{1}$$

where ΔV_d is the averaged voltage contribution due to the dead-time t_d over the switching period T_c, $\Delta V_d = t_d / T_c \, V_{dc}$.

It is assumed that the system is balanced in further analysis. The effects on three-phase inverters can be emphasized

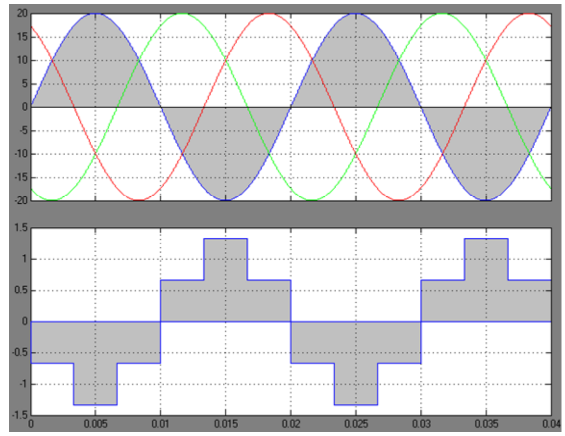

Fig. 2 Currents i_k (top) and load voltage error u_1 (bottom, normalized with respect to ΔV_d) for three-phase inverters

on the basis of the actual load voltage v_k expressed by pole voltages:

$$v_k = e_k - (e_1 + e_2 + e_3)/3 \tag{2}$$

Introducing in (2) the actual pole voltages (1) leads to:

$$v_k = v_k^* + u_k \,, \tag{3}$$

being v_k^* the reference load voltage:

$$v_k^* = e_k^* - \left(e_1^* + e_2^* + e_3^*\right)/3 \,, \tag{4}$$

and u_k the average load voltage error introduced by dead-time:

$$u_k = \Delta V_d \left\{-sign(i_k) + [sign(i_1) + sign(i_2) + sign(i_3)]/3\right\} \tag{5}$$

The time diagram u_k(t) is depicted in Fig. 2 for the first phase (k=1), considering three-phase sinusoidal balanced load currents, being $\omega_o = 2\pi/T$. In this case, the harmonics content of load voltage error developed as Fourier series, as also mentioned in [11], is:

$$\begin{aligned} u_k = -\Delta V_d \frac{4}{\pi} \Bigg\{ & \sin\left[\omega_o t - (k-1)\frac{2\pi}{3}\right] + \frac{1}{5}\sin\left[5\left(\omega_o t - (k-1)\frac{2\pi}{3}\right)\right] \\ & + \frac{1}{7}\sin\left[7\left(\omega_o t - (k-1)\frac{2\pi}{3}\right)\right] + \frac{1}{11}\sin\left[11\left(\omega_o t - (k-1)\frac{2\pi}{3}\right)\right] \\ & + \frac{1}{13}\sin\left[13\left(\omega_o t - (k-1)\frac{2\pi}{3}\right)\right] + \frac{1}{17}\sin\left[17\left(\omega_o t - (k-1)\frac{2\pi}{3}\right)\right] + \ldots \Bigg\} \end{aligned} \tag{6}$$

3. EFFECTS OF THE OUTPUT CURRENT RIPPLE

If the output current is with ripple, the effect of dead-times is reduced since during the zero crossings the average of sign function of current is zero, so there is no effect on specific pulses of pole voltage at zero crossings. More specifically, it can be shown that dead-time doesn't affect the width of the pole voltage pulse if the current turns from negative to positive during the voltage pulse. On Fig. 3 are shown the phase currents without and with ripple and the corresponding dead-time instantaneous voltage error (the dashed line is the average), obtained by simulations. It can be noticed that on first figure on left there is continuous dead-time effect. In second case (on the right) around zero crossing there are no dead-time effects, since the current always changes sign from negative to positive (Fig. 4) during the pole voltage pulse. The result when current changes sign from negative to positive during the pulse is that actual pulse is equal to reference one. On Fig. 5 is depicted the current with peak-to-peak envelope of ripple and averaged pole voltage error due to dead-time, taking into account the zero crossings. This effect on pole voltage can be summarized with a modified sign function $\underline{sign}(i_k)$, having zero values corresponding to multiple zero crossing interval of the current.

The load voltage error is still calculated using (1) and (5) but taking into account modified sign function:

$$e_k = e_k^* - \underline{sign}(i_k)\Delta V_d \tag{7}$$

as:

$$u_k = \Delta V_d\left\{-\underline{\mathrm{sign}}(i_k) + [\underline{\mathrm{sign}}(i_1) + \underline{sign}(i_2) + \underline{sign}(i_3)]/3\right\}. \tag{8}$$

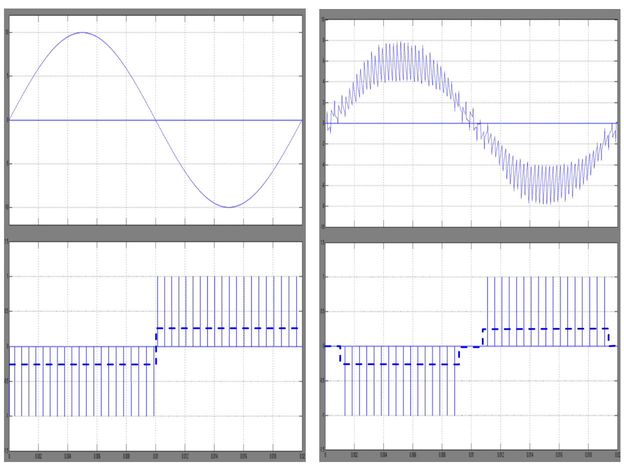

Fig. 3 Current i_k (top) and dead-time pole voltage error (bottom) for three-phase VSI with currents without ripple (left) and with ripple (right)

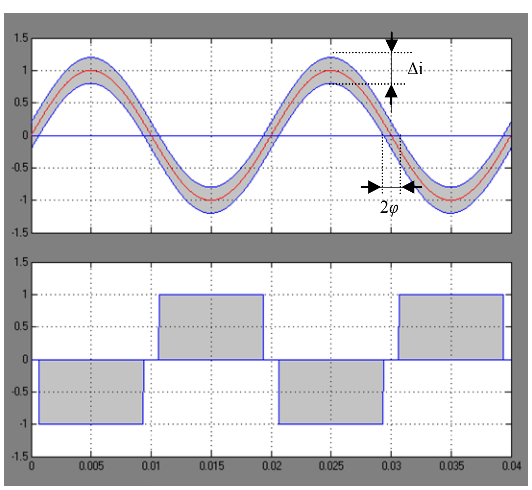

Fig. 5 Current i_k with peak-to-peak envelope of ripple (top) and modified sign function (bottom)

The average load voltage error is depicted on Fig. 6 for the first phase (u_1). The waveform of u_k can be seen as the sum of two contributions: the sign of the k-th leg current $-\underline{sign}(i_k)$ and average of signs of all output currents $1/3\Sigma\underline{sign}(i_k)$, considering modified sign functions. This two contributions are depicted in Fig. 7. The first one corresponds to unity square wave signal with period T, but modified with taking into account the zero values due to zero crossings, and the second one corresponds to a square wave signal, also modified, with amplitude $1/n$ and period T/n.

The Fourier development of the load voltage error can be obtained as a combination based on these two signals for the three-phase inverters, leading to:

$$\begin{aligned} u_k = \Delta V_d \frac{4}{\pi}\Big\{ & -\cos\varphi \sin\left[\omega t-(k-1)\frac{2\pi}{3}\right]-\frac{1}{3}\cos(3\varphi)\sin\left[3\left(\omega t-(k-1)\frac{2\pi}{3}\right)\right]- \\ & -\frac{1}{5}\cos(5\varphi)\sin\left[5\left(\omega t-(k-1)\frac{2\pi}{3}\right)\right]-\ldots+\frac{1}{3}\cos(3\varphi)\sin\left[3\left(\omega t-(k-1)\frac{2\pi}{3}\right)\right]+ \\ & +\frac{1}{9}\cos(9\varphi)\sin\left[9\left(\omega t-(k-1)\frac{2\pi}{3}\right)\right]+\frac{1}{15}\cos(15\varphi)\sin\left[15\left(\omega t-(k-1)\frac{2\pi}{3}\right)\right]+\ldots\Big\} \end{aligned} \tag{9}$$

where $\omega_o = 2\pi/T$ is the fundamental frequency and φ is the angle corresponding to half of the multiple zero crossing period of the current.

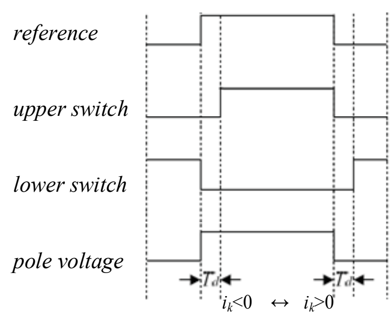

Fig. 4 Switching patterns and output pole voltage

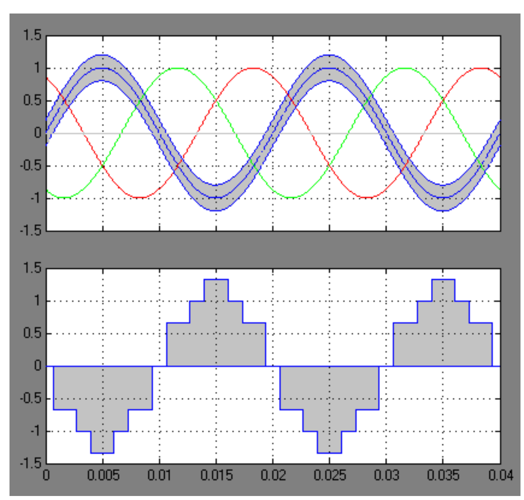

Fig. 6 Currents i_k (top) and load voltage error u_1 (normalized with respect to ΔV_d , bottom) for three-phase inverter in case of current with ripple

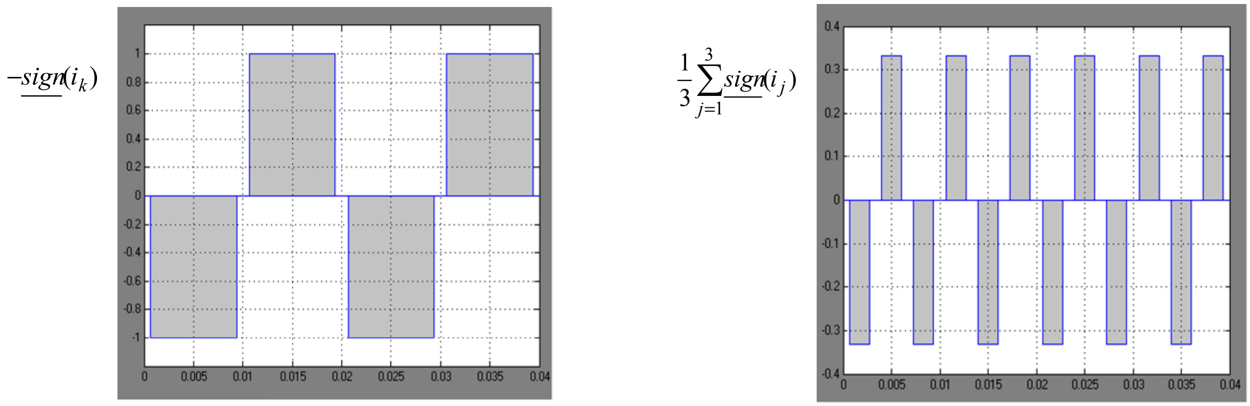

Fig. 7 Waveforms of the two contributions to the voltage error u_k normalized with respect to ΔV_d

It can be noticed that all harmonic components of the second signal completely erase with corresponding harmonics of the first signal, leading to the following simplified expression:

$$u_k = -\Delta V_d \frac{4}{\pi}\sum_{h=1}^{\infty}\frac{1}{h} cos(h\varphi)\, sin\left[h\left(\omega_o t-(k-1)\frac{2\pi}{3}\right)\right]. \quad (10)$$

The amplitude of harmonics is calculated according to (10):

$$U_h = \frac{4}{\pi}\frac{1}{h}\Delta V_d\, cos(h\varphi),\ (h \text{ odd integer not multiple of } n) \quad (11)$$

The amplitude of fundamental voltage error is given by (11) having $h = 1$:

$$U_1 = \frac{4}{\pi}\Delta V_d\, cos(\varphi)\,. \quad (12)$$

The output voltage error depends on the current polarity, which is a function of the load power factor angle ϕ. Defining the amplitude of the output voltage reference V^* as function of modulation index m as:

$$V^* = mV_{dc}\,, \quad (13)$$

enables calculation of the fundamental of the load voltage V on the basis of the load power factor angle as [1]:

$$V = -U_1\cos\phi + \sqrt{V^{*2} - U_1^2 \sin^2\phi}\,. \quad (14)$$

From (14) is possible to evaluate the amplitude of fundamental voltage error as:

$$U_1\Big|_{1,2} = \frac{-2V\cos(\phi) \pm \sqrt{4V^2\cos^2\phi + 4(V^{*2}-V^2)}}{2}\,, \quad (15)$$

where just one solution is acceptable. Eq. (15) can be used with simulation results to calculate U_1 on the basis of V^*, V, and $\cos\phi$. This value is compared to the one given by (12).

In order to verify what is the effect of dead-time on output voltages, of interest is the value of multiple zero crossing time interval (angle) of output currents. As the first order of approximation, the amplitude of current ripple, Δi, can be evaluated as in [13], [14]:

$$\Delta i = \frac{V_{dc}T_c}{8L}\,. \quad (16)$$

The current ripple evaluated by (16) applies only to case with maximum modulation index. It has been verified with simulations that the current ripple and modulation index are almost linearly dependent in the range 0.1-0.5, so it is possible to modify (16) as follows:

$$\Delta i = 2m\frac{V_{dc}T_c}{8L}\,. \quad (17)$$

Eq. (17) is just a simple approximation to evaluate the current ripple amplitude, but is has been numerically verified it is accurate enough to get reasonable results within the goals of this paper.

According to Fig. 5, the angle corresponding to zero crossings of the current can be evaluated as:

$$\varphi = arcsin\left(\frac{\Delta i/2}{I_{fund}}\right), \quad (18)$$

where I_{fund} is the fundamental output current amplitude.

4. NUMERICAL RESULTS

In order to verify the theoretical developments shown in previous sections, circuit simulations are carried out by SimPowerSystems of Matlab considering a three-phase VSI supplying RL load with low power angle at f = 50 Hz. The dead-time duration is t_d = 20 µs, the switching frequency is $1/T_c$ = 2 kHz, and the dc voltage supply is V_{dc} = 200 V. Different values of modulation index m are investigated (0.1, 0.2, 0.45). The harmonic spectrum of the voltage error is shown in all cases up to 19th harmonic component.

First of all, in order to emphasize the mismatch introduced by a relevant current ripple, in Fig. 8 are compared the two cases of sinusoidal output current (Fig. 8a) and output current with ripple (Fig. 8b) having the same power factor and the same fundamental amplitude. In both cases, the black columns at left side show the voltage error harmonics calculated by theory as shown in [9], considering pure sinusoidal output currents with load power factor

PF=0.992. In Fig. 8a harmonics are obtained considering different modulation indexes (m = 0.1, 0.2, 0.45, columns from left to right side) and same power factor. In Fig. 8b harmonics are obtained with the output current ripple corresponding to a passive RL load, having R=5Ω and L=2mH, with different modulation indexes (m = 0.1, 0.2, 0.45, columns from left to right side).

As expected from the theory, only odd-order harmonics appear and harmonics with order multiple of three are practically missing (i.e., 3rd, 9th, 15th), according to (6) and (9). It can be noticed that in Fig. 8a the theoretical value considering theoretical approach [9] with single current zero crossing, is in good agreement with simulations obtained with sinusoidal output currents. Figure 8b shows mismatches between the theoretical values considering single zero crossing of currents and simulation results obtained with passive RL load, that corresponds to an output current ripple that can not be neglected.

Figure 9 shows the numerical results compared with the proposed method to account for the effects of the current ripple. In particular, in Fig. 9 are shown 4 different cases considering 4 different values of inductance (2, 3, 5 and 10 mH), and for each one considering different value of modulation index (m = 0.1, 0.2, 0.45, columns from left to right side). The black columns represent the harmonic amplitudes given by theory, according to section 3, considering the theoretical approach introduced in this paper, calculated for every value of L. The other columns correspond to harmonic amplitudes introduced by simulation with passive RL load with different values of modulation index (columns from left to right side). It can be noticed that simulation results are in good agreement with the proposed theoretical approach, almost in all cases.

5. CONCLUSION

The switching time delay in a PWM inverter has effects on inverter operation. It causes a decrease in the fundamental component of load voltages and introduces low-order harmonics. It is shown that, despite PWM methods that produce sinusoidal outputs, free from any lower order harmonics, inverter dead-time generates odd low order harmonics. This is important in all cases in which the output voltage is set in open-loop or it is evaluated on the basis of dc voltage and switching pattern.

In this paper the dead-time effects on inverter output variables has been analyzed in three-phase inverters with output currents with relevant ripple. It has been shown that due to multiple zero crossings of current, dead-time effect is reduced, and there is different voltage harmonic spectrum with respect to one which considers pure sinusoidal output currents. A simplified theoretical approach is proposed to evaluate the value of time interval when the zero crossings occur, on which is based the theoretical analysis of the effect of dead-time on output voltage distortion. Further on, this analytical developments have been compared with numerical results obtained by circuit simulations, showing a good agreement. Experimental results are currently in progress.

6. REFERENCES

[1] Seung-Gi Jeong and Min-Ho Park, "The Analysis and Compensation of Dead-Time Effects in PWM Inverters," *IEEE Trans. on Ind. Electronics*, vol. 38, no. 2, April 1991, pp. 108-114.

[2] D. Leggate, R.J. Kerkman, "Pulse-based dead-time compensator for PWM voltage inverters," IEEE Trans. on Industrial Electronics, vol. 44, no. 2, April 1997, pp. 191-197.

[3] T. Sukegawa, K. Kamiyama, K. Mizuno, T. Matsui and T. Okuyama, "Fully Digital, Vector-Controlled PWM VSI-Fed ac Drives with an Inverter Dead-Time Compensation Strategy," *IEEE Trans. on Ind. Appl.*, vol. 21, no. 3,May/June 1991, pp. 552-559.

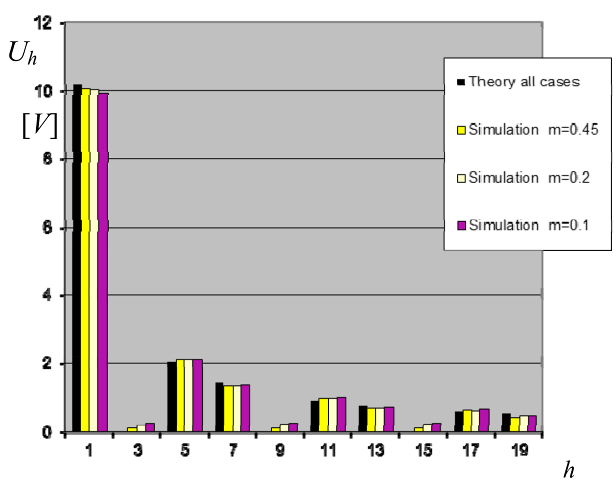

(a) Pure sinusoidal currents (PF=0.992)

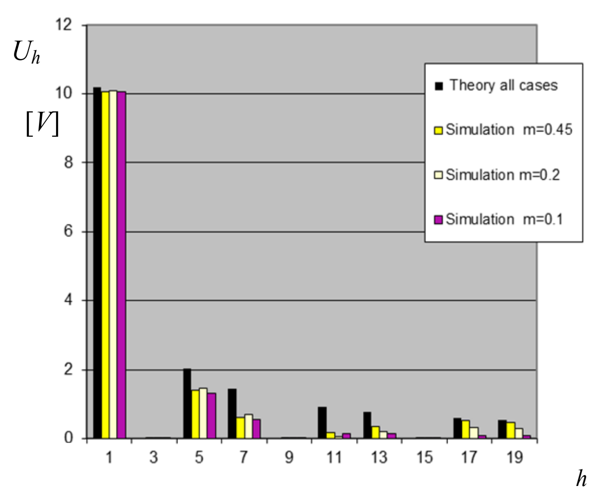

(b) Currents with ripple: R=5Ω, L=2mH (PF=0.992)

Fig. 8 Harmonic spectrum of voltage error obtained by theory (black) and simulated: (a) with pure sinusoidal currents (b) with current with ripple, for different modulation indexes

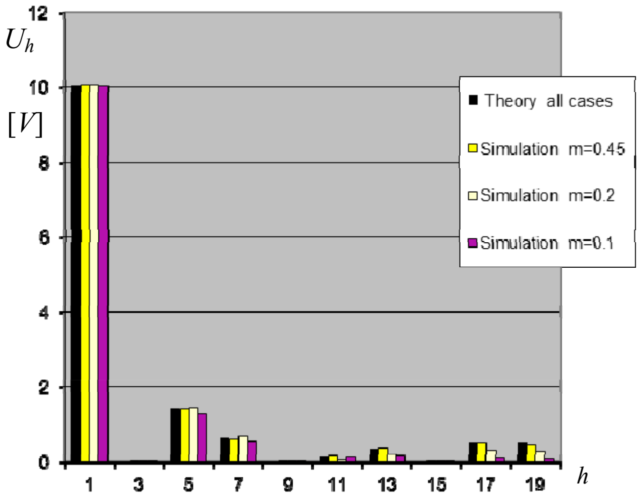

(a) Currents with ripple: R=5Ω, L=2mH

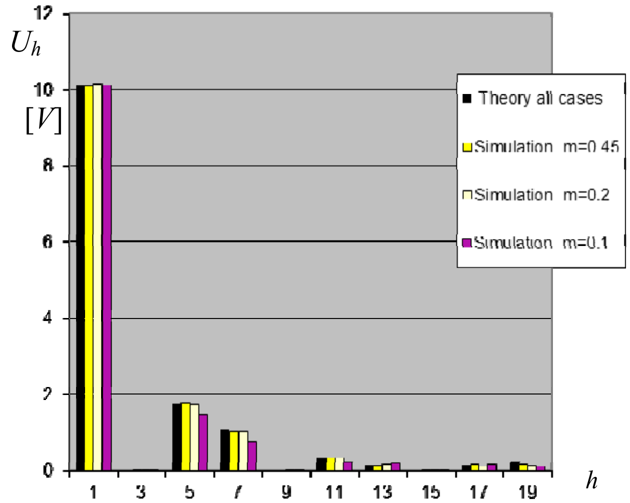

(b) Currents with ripple: R=5Ω, L=3mH

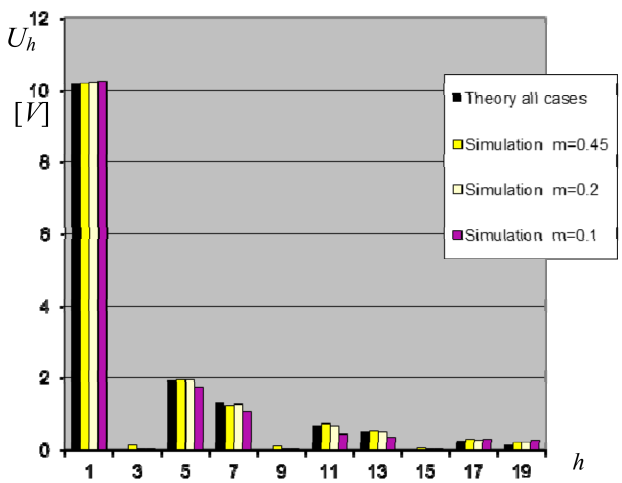

(c) Currents with ripple: R=5Ω, L=5mH

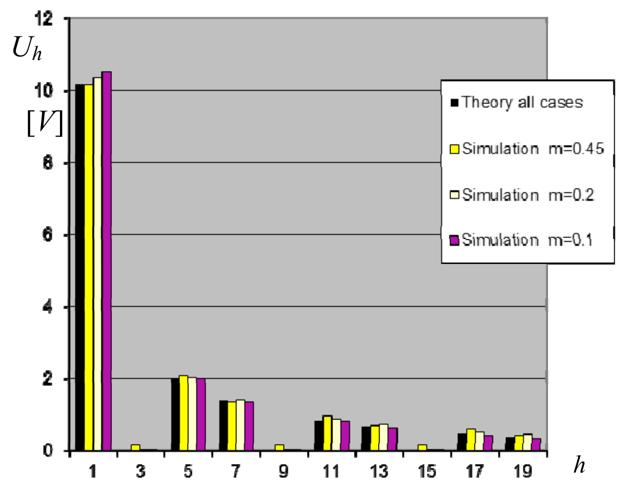

(d) Currents with ripple: R=5Ω, L=10mH

Fig. 9 Harmonic spectrum of voltage error obtained by new theoretical approach and simulated with current with ripple (different values of L)

[4] A. Muiioz-Garcia T.A. Lipo, "On-line dead time compensation technique for open-loop PWM-VSI drives," *proc. of 13th Applied Power Electronics Conference and Exposition*, APEC, vol. 1, Feb 1998, pp. 95-100.

[5] L.Chen, F.Z.Peng "Dead-time elimination for voltage source inverters," *IEEE Trans. on Power Electronics*, vol. 23, no. 2, March 2008, pp. 574-580.

[6] E.Levi, R.Bojoi, F.Profumo, H.A.Toliyat, S.Williams on "Multiphase induction motor drives – a technology status review," *IET Electr. Power Appl.*, vol. 1, no. 4, July 2007, pp. 489-516.

[7] M.Jones, D.Dujic, E.Levi S.N.Vukosavic, "Dead-Time Effects in Voltage Source Inverter Fed Multi-Phase AC Motor Drives and Their Compensation," *in Proc. of 13th European Conf. on Power Electronics and Applic.*, EPE, Barcelona (Spain), 8-10 Sept. 2009.

[8] K. Oka, H. Enokijima, H. Kubota, K. Matsuse, "Analysis and Compensation Method of Voltage Error by Dead-Time with Five-Leg Inverter for Two-AC Motor Independent Drives," *in Proc. of Energy Conversion Congress and Expositions*, IEEE-ECCE, San Jose-CA (USA), Sept. 20-24, 2009, pp. 869-876.

[9] G. Grandi, J. Loncarski, "Analysis of Dead-Time Effects in Multi-phase Voltage Source Inverters," proc. of 6th IET Conf. on Power Electronics, Machines and Drives, PEMD 2012, Bristol (UK), march 27-29, 2012.

[10] G. Grandi, J. Loncarski, "Space Vector Analysis of Dead-Time Voltage Distortion in Multi-phase Inverters", accepted for EPE-PEMC, ECCE Europe Conference, Novi Sad (RS), Sept. 4-6, 2012.

[11] S.H. Hwang and J.M. Kim, "Dead Time Compensation Method for Voltage-Fed PWM Inverter," *IEEE Transactions on energy conversion*, vol. 25, no. 1, March 2010, pp. 1-10.

[12] Zixin Li; Ping Wang; Yaohua Li; Congwei Liu; Haibin Zhu, "Dead-time compensation for VSI based power supply with small filter inductor," *Power Electronics and Motion Control Conference, 2009. IPEMC '09. IEEE 6th International*, 2009, pp. 1519- 1523

[13] D. Dujic, M. Jones, E. Levi "Analysis of Output Current Ripple rms in Multiphase Drives Using Space Vector Approach," IEEE Transactions on power electronics, vol. 24, no. 8, March 2009

[14] J.W. Kolar, H. Ertl, F.C Zach, "Minimization of the harmonic RMS contents of the mains current of a PWM converter system based on the solution of an extreme value problem," Proc. Int. Conf. on Harmonics in Power Systems, ICHPS, Budapest (HU), 1990.